Desalination and Water Treatment
www.deswater.com

doi: 10.5004/dwt.2017.21601

97 (2017) 225–233
November

Comparative study on the electrocatalytic performance of different catalysts supported on activated carbon particle electrodes in a three-dimensional electrode cell

Gui-Ping Cao*, Ya-Feng Zhuang, Li Wang

Department of Chemical Engineering, Changzhou Institute of Technology, Changzhou 213032, China, emails: caogpczu@163.com (G.-P. Cao), zhuangyf@czu.cn (Y.-F. Zhuang), wangli@czu.cn (L. Wang)

Received 20 May 2017; Accepted 31 October 2017

ABSTRACT

The electrocatalytic performance of different catalysts loaded on activated carbon particle electrodes via an impregnation method was investigated through the degradation of methyl orange in a three-dimensional electrode cell. Mn, Co, Zn, Sn, and Sb catalysts were chosen to study the electrocatalytic performance of single-component catalysts. The results indicated that 0.4 mol/L Mn and 0.2 mol/L Sb catalysts exhibited excellent electrocatalytic activities, whereas the electrocatalytic performance of 0.6 mol/L Zn catalyst was the worst among the catalysts investigated. The electrocatalytic performance of single-component catalysts was related to their concentrations and structures. The electrocatalytic performance of double-component catalysts, Co–Mn, Sn–Mn, and Sb–Mn, was also investigated. Compared with the single-component catalyst Mn, the degradation half-life with the Sn–Mn and Sb–Mn catalysts decreased from 11.3 to 7.4 min and 5.1 min, respectively. In contrast, the half-life with the Co–Mn catalyst increased from 11.3 to 14.9 min. The combination of two catalytic components produced synergetic or antagonistic effects on the electrocatalytic performance of the resulting double-component catalyst. The triple-component catalyst, Sn–Sb–Mn, did not further improve the electrocatalytic performance of the corresponding double-component catalysts because of agglomeration occurring at the electrode surface. The incorporation of an excessive amount of components was not conducive to enhancing the electrocatalytic performance of catalyst. The possible mechanism for the differences in the electrocatalytic performance of different catalysts was discussed in detail.

Keywords: Electrocatalytic performance; Single-component catalyst; Double-component catalyst; Triple-component catalyst; Particle electrodes

1. Introduction

Electrochemistry offers several promising approaches that, in many cases, can be employed in "green" processes that prevent pollution problems [1]. Powerful redox reagents (e.g., hydroxyl radicals, hypochlorite, ozone, and metal redox couples) are produced in electrochemical reactions, and these reagents can oxidize a host of organic pollutants [2]. Thus, the technique has been widely applied to the treatment of textile wastewater [3], tannery wastewater [4], pigment wastewater [5], bilge wastewater [6], and municipal wastewater [7].

The electrochemical technology based on a three-dimensional electrode has been attracting significant attention and interest because it can yield treatment efficiency higher than that provided by a conventional two-dimensional electrode because of its greater surface area-to-volume ratio [8]. Three-dimensional electrode technology has been used to degrade landfill leachate [9], real dyeing wastewater [10], refinery wastewater [11], coking wastewater [12], and paper-mill wastewater [13]. Compared with those of a conventional two-dimensional electrode, the primary characteristic of the three-dimensional electrode is that numerous small particles placed in the three-dimensional electrode system form charged microelectrodes under the influence of an electric field; such electrodes are referred to as particle electrodes. The observed

---

* Corresponding author.

1944-3994/1944-3986

higher efficiency of the three-dimensional electrode has been attributed to the larger specific surface area produced by particle electrodes [11]. This characteristic of particle electrodes has played an important role in allowing researchers to estimate the performance of the total system [14].

The development of efficient particle electrodes is key for overcoming the high-cost bottleneck in the electrochemical treatment of wastewater. Recently, carbon nanotube (CNT) particle electrodes have been reported to be effective in the treatment of wastewater and can be considered as a new type of three-dimensional particle electrodes [15]. The main advantage of CNT particle electrodes is their ability to facilitate contaminant mass transfer from the bulk solution to the electrode surface; this ability stems from the enhanced surface area of these electrodes, which often leads to higher reaction rates [16]. A novel mesoporous carbon material, carbon aerogel (CA), has been prepared for use as the particle electrode in a three-dimensional electrode cell [17]. CA exhibits numerous exceptional properties, such as low mass density, continuous porosity, high surface areas, and high electrical conductivity [18]. However, the techniques for preparing these particle electrodes are complicated, which is not conducive to its application.

The most commonly used particle electrode material is activated carbon (AC), and electrodes based on this material have been used to effectively treat pollutants [19,20]. The performance of AC electrodes can be attributed to the good adsorbability and electroactivity of AC under electrochemical conditions [21]. At the same time, it is also one of the most common carriers for catalysts [22,23]. The supporting of catalysts on particle electrodes provides one alternative to enhance the specific surface area of the electrode and promote mass transfer, which is one of the limitations in a two-dimensional system [24]. In a three-dimensional electrode cell, catalysts on particle electrodes undergo different heterogeneous reactions, of which Fenton and Fenton-like reactions are the most promising [25]. In addition to iron, other transition metals can also exhibit catalytic activity toward Fenton-like reactions, such as manganese, nickel, and cobalt [26–28]. Some rare metals (e.g., Sn and Sb) are also good catalysts for the degradation of organic compounds. The electrocatalytic performance of Sb_2O_3/AC particles is superior to that of AC particle electrodes [29]. However, to the best of our knowledge, very little work has studied the difference in electrocatalytic performance of different catalysts supported on particle electrodes.

In this paper, several economical and widely used catalysts were chosen and loaded onto AC particle electrodes using an impregnation method. We systematically investigated the electrocatalytic performance of single- and multiple-component catalysts through the degradation of methyl orange in a three-dimensional electrode cell and analyzed the reasons for the difference in electrocatalytic activity of catalysts by characterizing the surfaces of the particle electrodes. This study may contribute to the development of efficient and practical particle electrodes.

2. Materials and methods

2.1. Materials

Granular AC with an average particle size of 5.6 ± 1 mm was purchased from Sinopharm Chemical Reagent Co., Ltd. (China) and used to fabricate particle electrodes. The AC was washed with boiling water four times and then dried at 373 K for approximately 4 h before use.

Manganese nitrate solution ($Mn(NO_3)_2$, 50%), cobalt nitrate hexahydrate ($Co(NO_3)_2\cdot 6H_2O$), zinc nitrate hexahydrate ($Zn(NO_3)_2\cdot 6H_2O$), tin chloride pentahydrate ($SnCl_4\cdot 5H_2O$), and antimony chloride ($SbCl_3$) were purchased from Shanghai Chemical Reagent Co., Ltd. (China) and were used as precursors for the preparation of Mn, Co, Zn, Sn, and Sb catalysts, respectively. All chemicals were of analytical grade, and each was prepared as a 2 mol/L stock solution. Working solutions with different concentration were freshly prepared by diluting the stock solution with water before use.

2.2. Loading of catalysts

One or more catalytic components were loaded onto AC particle electrodes using an impregnation method. Approximately 10.00 g of dry AC particles was immersed into 100.0 mL of a working solution and oscillated by a shaker at 150 rpm for 3.5 h. The working solutions used in the immersing process included one, two or three components of $Mn(NO_3)_2$, $Co(NO_3)_2\cdot 6H_2O$, $Zn(NO_3)_2\cdot 6H_2O$, $SnCl_4\cdot 5H_2O$, and $SbCl_3$. After impregnation, the AC particles were dried by being heated at 353 K for 2 h and were subsequently calcined at 673 K for 3.5 h. The same procedure was repeated once again, and the corresponding catalyst was loaded onto particle electrodes.

2.3. Determination of electrocatalytic performance

The electrocatalytic performance of the catalysts supported on AC particle electrodes was evaluated by degradation of methyl orange in a three-dimensional electrode cell, shown in Fig. 1. The cell was constructed of plastic and had dimensions of 15 cm × 8 cm × 6 cm. The stainless steel anode and cathode (main electrodes) were situated 4.4 cm apart, and 10.00 g particle electrodes loaded with a catalyst were packed between the two main electrodes. A magnetic stirrer stirred the methyl orange solution at 800 rpm. Prior to electrolysis, the particle electrodes were first soaked in methyl orange solution for 24 h to avoid adsorption effects. During electrolysis, the potential of 9 V used in this study

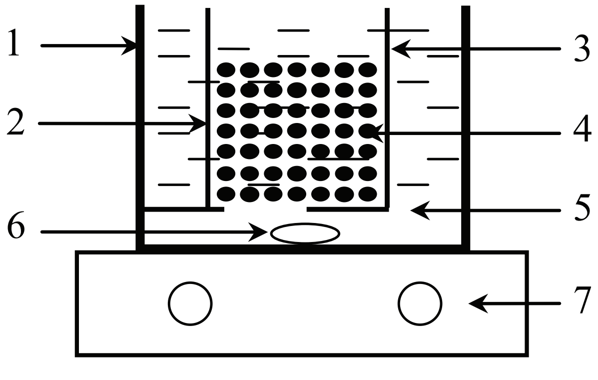

Fig. 1. Schematic diagram of a three-dimensional electrode cell. 1: support, 2: anode, 3: cathode, 4: particle electrode, 5: micropore plate, 6: magnetic stirrer, and 7: magnetic stirring apparatus.

was controlled by a DC power supply. 200 mL of 10.0 mg/L methyl orange solution was used in each test, and 12 g/L Na_2SO_4 was added to the methyl orange solution as an electrolyte. The treated solution was then subjected to analysis of the remaining methyl orange concentration at selected electrolysis time intervals.

2.4. Analytical method and calculation

The concentration of methyl orange remaining in the solution after electrolysis was determined with a UV 1102 spectrophotometer. The analytic wavelength selected for the absorption measurement was 463 nm. The absorbance of solution at 463 nm was proportional to the methyl orange concentration in the range from 0.8 to 10.0 mg/L, and the standard curve equation was as follows:

$$A = 0.0723c - 0.012 \tag{1}$$

where A was the absorbance of solution, c represented the methyl orange concentration (mg/L). The decolorizing efficiency was calculated as follows:

$$\text{Decolorizing efficiency (\%)} = \frac{c_0 - c_t}{c_0} \times 100 \tag{2}$$

where c_0 was the initial methyl orange concentration and c_t was the residual methyl orange concentration after degradation time t (min). The degradation rate of methyl orange was closely related to the electrocatalytic performance of the catalyst in the whole electrolysis process. The concentration of methyl orange in the degradation process with different catalysts followed a first-order kinetic equation well, and the rate constant was obtained by using the corresponding regression equation, as shown in Eq. (3):

$$\ln(c_t/c_0) = -kt \tag{3}$$

where k was the degradation rate constant, and t was the degradation time.

The slope of the linear regression line of $\ln(c_t/c_0)$ against time gave the degradation rate constant. The half-life ($t_{1/2}$) was determined by Eq. (4):

$$t_{1/2} = \ln 2/k \tag{4}$$

The surface morphologies of the particle electrodes were characterized by scanning electron microscopy (SEM, Carl Zeiss SUPRA55). The specimens were sprayed with gold prior to analysis. The phase structure of the particle electrodes was examined by X-ray diffraction (XRD), which was performed on a Rigaku D/max 2500PC diffractometer equipped with a Cu-Kα radiation source that was operated at 60 kV and 300 mA. In addition, the elemental compositions of particle electrodes were determined by energy-dispersive spectrometry (EDS), which was performed using an Oxford unit attached to the scanning electron microscope.

3. Results and discussion

In a three-dimensional electrode cell, oxidation of organic matter could be classified as direct oxidation at surface of anode and particle electrodes and indirect oxidation distant from the electrode surface [30]. The degradation of methyl orange depended on electrolysis reaction parameters and electrode types. The surface and material of particle electrodes greatly influenced the process. Electrocatalytic oxidation mainly used free radicals produced by a catalyst attached on particle electrodes under an electric field to oxidize methyl orange. The decolorizing efficiency of methyl orange was closely related to the electrocatalytic performance of the catalyst.

Five catalysts are investigated in this study: the transition metals Mn, Co, and Zn, which are in the fourth period of the periodic table of the elements, and rare metals Sn and Sb, which are in the fifth period of the periodic table of the elements. Although iron is also a commonly used catalyst, it is not investigated in the present work to avoid interference produced by a typical Fenton reaction [31].

3.1. Electrocatalytic performance of single-component catalysts

To compare the electrocatalytic performance of single-component catalysts, we investigate the effect of the concentration of different single-component catalysts on degrading methyl orange, and the results are shown in Fig. 2. A greater decolorizing efficiency indicates better electrocatalytic performance of the catalyst. The electrocatalytic performance of each of the investigated catalyst was closely related to its concentration. As evident in the results in Fig. 2, the optimal concentrations of the Mn, Co, Zn, Sn, and Sb catalysts were 0.4, 0.6, 0.6, 0.8, and 0.2 mol/L, respectively, and their corresponding decolorizing efficiencies reached 72.0%, 53.8%, 45.9%, 64.5%, and 65.2%, respectively. When the catalyst loading was excessive, some H_2O_2 molecules produced during the electrolysis process were decomposed into oxygen and water at the catalyst surface before the organic molecules were degraded [32], which inhibited the degradation of methyl orange. Therefore, high catalyst loadings were not conducive to improving the catalysts' electrocatalytic activity.

The presence of chloride ions seems to enhance the decolorizing efficiency of organic pollutants [33]. According to the EDS composition analysis, the chlorine content in particle electrodes loaded with 0.8 mol/L Sn catalyst was approximately 1.97%, whereas that in particle electrodes loaded with 0.2 mol/L Sb catalyst was approximately 2.83%, which was 1.44 times greater than that in the former case. However, their decolorizing efficiencies were very similar. Furthermore, the decolorizing efficiency of particle electrodes did not increase when the Sb catalyst concentration was increased from 0.6 to 1.0 mol/L. Therefore, the effect of chlorine attached to the particle electrodes on the catalysts' electrocatalytic performance could be ignored in this study.

According to the data measured above, the electrocatalytic performance of the fifth-period metal catalysts was superior to that of catalysts in the fourth period. The electron transfer plays a critical role in the electrocatalytic process [34]. The enhancement of heterogeneous electron transfer can cause electrodes to exhibit high electrocatalytic oxidation [35]. Therefore, palladium (a fifth-period catalyst) and iridium (a sixth-period catalyst) are used to improve the performance of electrodes [36,37]. However, the electrocatalytic performance of different metal catalysts in the same period

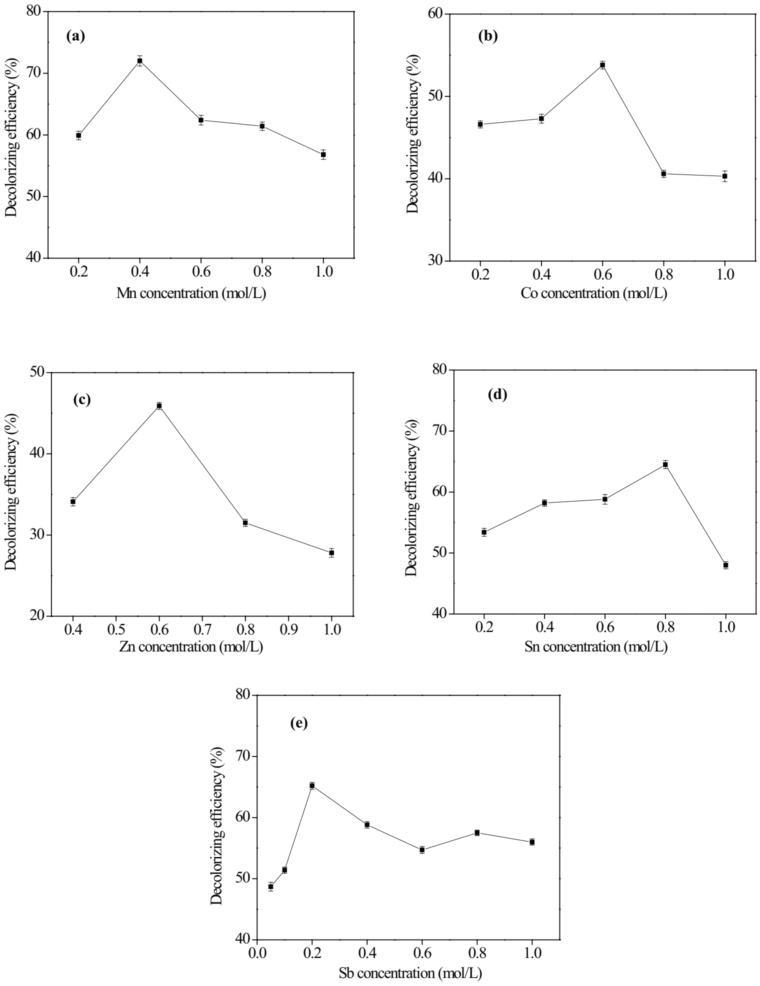

Fig. 2. Effects of single-component catalyst concentration on the decolorizing efficiency of particle electrodes: (a) Mn catalyst, (b) Co catalyst, (c) Zn catalyst, (d) Sn catalyst, and (e) Sb catalyst. Experimental condition: 10.00 g particle electrode dose, 200 mL of 10.0 mg/L methyl orange solution, 12 g/L Na_2SO_4, 9 V cell voltage, 20 min electrolysis time and repeated three times.

was not completely consistent. The decolorizing efficiency with 0.8 mol/L Sn catalyst was almost the same as that with 0.2 mol/L Sb catalyst, and the Sb catalyst exhibited better electrocatalytic activity. Therefore, the electrocatalytic activity of metal catalysts had also been suggested to depend on the number of unpaired electrons in the metal atom because unpaired electrons facilitated chemical bond breaking of organic compounds during electrochemical oxidation [38]. This conclusion was also confirmed from the other three catalysts (Mn, Co, and Zn) in the fourth period. The electrocatalytic performance of the Mn catalyst with five unpaired electrons was the strongest, whereas the electrocatalytic performance of Zn catalyst without unpaired electrons was the weakest.

The time course variation in normalized concentration of methyl orange and its dependence on single-component catalysts are illustrated in Fig. 3. The amount of degradation was closely related to the type of single-component catalysts. Based on the concentration data in Fig. 3, the electrocatalytic degradation of methyl orange with different catalysts was found to fit the first-order kinetic model well (Eq. (3)). The degradation rate constants and half-life values, including

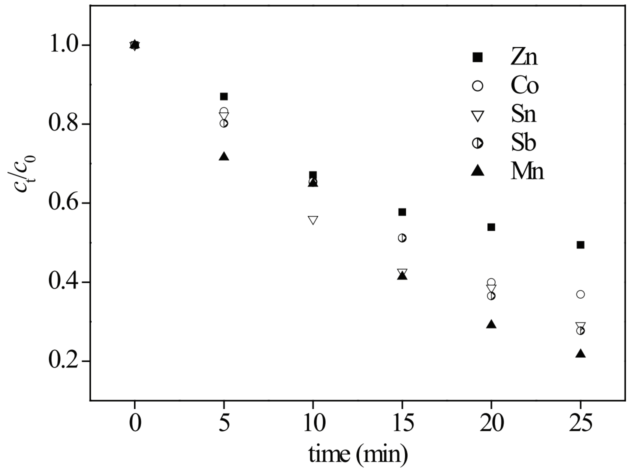

Fig. 3. Variation of normalized methyl orange concentration as a function of degradation time with different single-component catalysts. Experimental condition: 10.00 g particle electrode dose, 200 mL of solution, c_0 10.0 mg/L methyl orange, 12 g/L Na_2SO_4, and 9 V cell voltage.

those of some experiments that will be described elsewhere in this paper, are presented in Table 1. Regression coefficient (R^2) was often >0.97 suggesting that the electrochemical degradation of methyl orange with different catalysts followed first-order kinetics in their concentrations. Mn and Sb catalysts exhibited excellent electrocatalytic activities according to catalyst concentration and degradation half-life. The degradation half-life was the shortest in the case of Mn, only 11.3 min; the concentration supported on particle electrodes was the lowest in the case of Sb, only 0.2 mol/L, and the half-life with this catalyst was 13.4 min. The results demonstrate that the electrocatalytic performance of the single-component catalysts was closely related to their concentration and structural features. The catalysts with more unpaired electrons and/or larger atomic radii exhibited greater electrocatalytic activity.

Fig. 4 shows the XRD patterns of particle electrodes with Mn and Sb catalysts. The diffraction peaks in Fig. 4(a) indicated that crystalline patterns were formed on the electrode surface during loading of the Mn catalyst. However, the diffraction peaks changed after the particle electrodes had been used. These changes indicated that the stability of the Mn catalyst on the electrode surface was poor and its electrocatalytic activity would be affected after it was used. In contrast, no diffraction peaks were apparent in the XRD patterns in Fig. 4(b). The Sb catalyst did not show crystalline patterns, indicating a good dispersion of this catalyst. In the experiments of degrading methyl orange for 10 times repeatedly, the decolorizing efficiency with the Sb catalyst maintained in the range from 60.6% to 65.2%, whereas that with the Mn catalyst showed a downward trend from 72.0% to 52.8%. The Sb catalyst exhibited stable performance.

3.2. Electrocatalytic performance of double-component catalysts

The effect of Zn component on the electrocatalytic performance of double-component catalysts was not studied because of its poor electrocatalytic activity. The electrocatalytic performance of three double-component catalysts based on Mn, that is, Co–Mn catalyst, Sn–Mn catalyst, and Sb–Mn catalyst, was investigated in detail.

Table 1
First-order kinetic parameters for the degradation of methyl orange with different catalysts supported on particle electrodes

Catalyst	Concentration (mol/L)	k (1/min)	R^2	$t_{1/2}$ (min)
Zn	0.6	3.23×10^{-2}	0.979	21.5
Co	0.6	4.25×10^{-2}	0.987	16.3
Sn	0.8	4.98×10^{-2}	0.981	13.9
Sb	0.2	5.16×10^{-2}	0.992	13.4
Mn	0.4	6.16×10^{-2}	0.983	11.3
Co–Mn	0.4:0.6	4.66×10^{-2}	0.973	14.9
Sn–Mn	0.8:0.4	9.42×10^{-2}	0.996	7.4
Sb–Mn	0.1:0.4	13.51×10^{-2}	0.992	5.1
(Sb–Mn)–Sn	0.1:0.4:0.8	4.60×10^{-2}	0.994	15.1
(Sn–Mn)–Sb	0.8:0.4:0.1	4.90×10^{-2}	0.982	14.1
Sn–Sb–Mn	0.8:0.1:0.4	6.36×10^{-2}	0.979	10.9

The effects of component concentration on the electrocatalytic performance of double-component catalysts are shown in Fig. 5. When the Mn concentration was 0.4 mol/L, the decolorizing efficiency of particle electrodes with Co–Mn catalyst reached a maximum value 56.9% with the addition of 0.4 mol/L Co (Fig. 5(a)). When the Co concentration was 0.4 mol/L, the decolorizing efficiency increased to 61.7% with the addition of 0.6 mol/L Mn, which was 10.3% less than the decolorizing efficiency achieved with the 0.4 mol/L Mn single-component catalyst. Therefore, the electrochemical performance of the Co–Mn catalyst could not be effectively improved by the combination of Mn and Co catalytic components. The decolorizing efficiencies of particle electrodes with Sn–Mn catalysts combined in different concentrations were greater than 81% (Fig. 5(b)), which was higher than that achieved with either Sn or Mn single-component catalyst. The decolorizing efficiency with Sn–Mn catalyst increased slightly with increasing concentration of the Mn component. However, if the amount of Mn component in the catalyst was partially substituted by that of Sn component, the decolorizing efficiency decreased from 85% to 81%. These results indicate that the content of each component affected the electrocatalytic activity of Sn–Mn catalyst. The decolorizing efficiency with Sb–Mn catalyst at different concentrations was stable

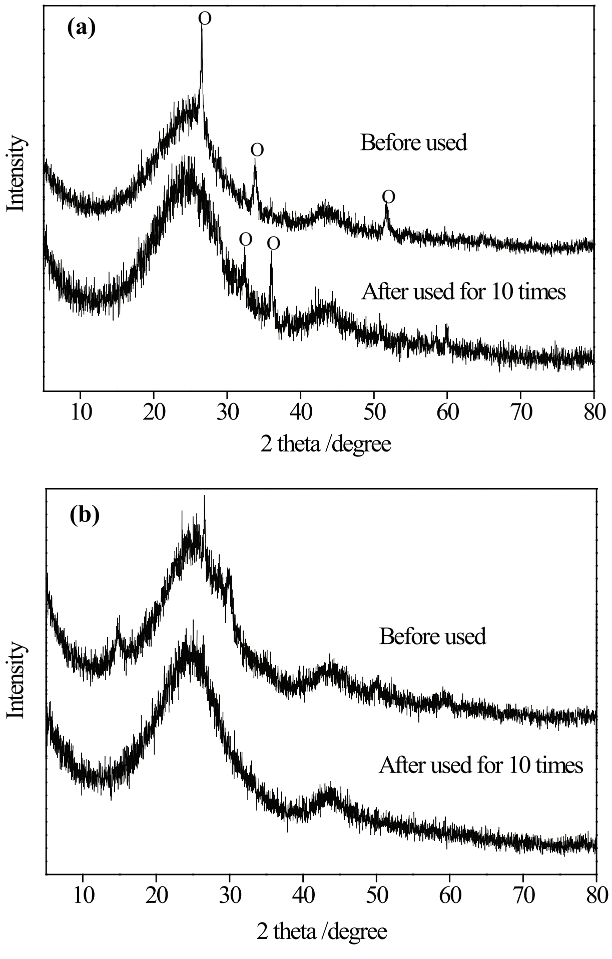

Fig. 4. XRD patterns of particle electrodes loaded with (a) Mn catalyst and (b) Sb catalyst.

and exceeded 87% (Fig. 5(c)), which was significantly higher than that achieved with either Sb or Mn single-component catalyst. Furthermore, in the process of degrading methyl orange repeatedly, the decolorizing efficiency with Sb–Mn catalyst remained within the range from 83.1% to 87.9%. The stability of the Sb–Mn catalyst was further confirmed by the corresponding XRD patterns shown in Fig. 6. The diffraction peaks in Fig. 6 almost did not change after the particle electrodes had been used for 10 times, which indicated that the addition of Sb component might improve the stability of the Mn catalyst. Therefore, the Sb–Mn catalyst exhibited both excellent electrocatalytic activity and good stability.

The concentration of methyl orange decreased exponentially with degradation time in the presence of the three double-component catalysts (Fig. 7). More than 80% methyl orange was degraded during 15 min electrochemical treatment with the Sb–Mn catalyst. Based on the kinetic analysis in Table 1, the addition of Sb component in the Sb–Mn catalyst resulted in a 54.8% reduction in the half-life compared with the Mn single-component catalyst. However, the half-life with the Co–Mn catalyst was 14.9 min, which was 1.4 min shorter than that with the Co single-component catalyst but

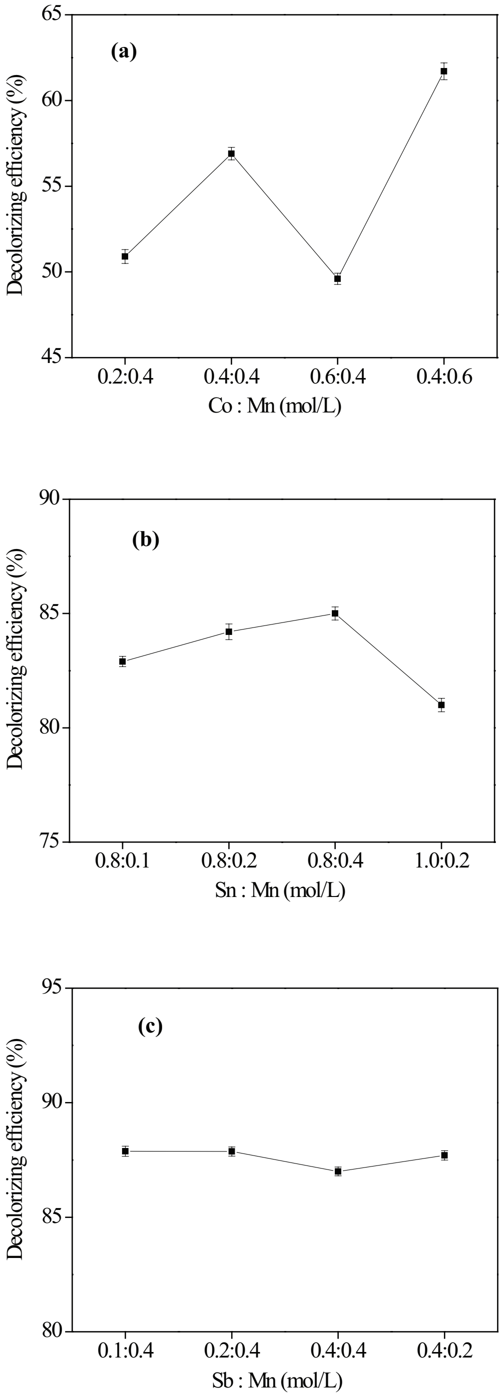

Fig. 5. Effects of component concentration on the decolorizing efficiency of double-component catalysts: (a) Co–Mn catalyst, (b) Sn–Mn catalyst, and (c) Sb–Mn catalyst. Experimental condition: 10.00 g particle electrode dose, 200 mL of 10.0 mg/L methyl orange solution, 12 g/L Na_2SO_4, 9 V cell voltage, 20 min electrolysis time and repeated three times.

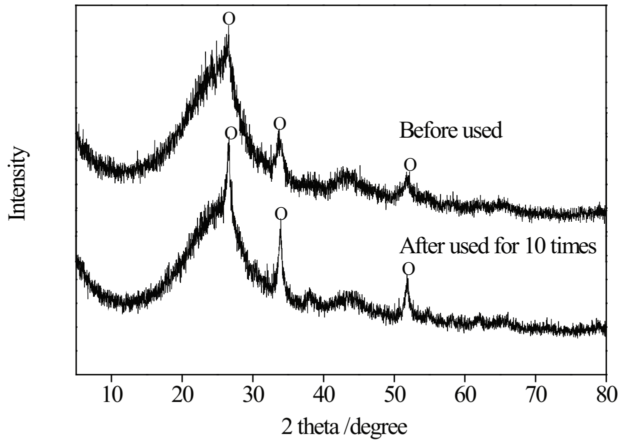

Fig. 6. XRD patterns of particle electrodes loaded with Sb–Mn catalyst.

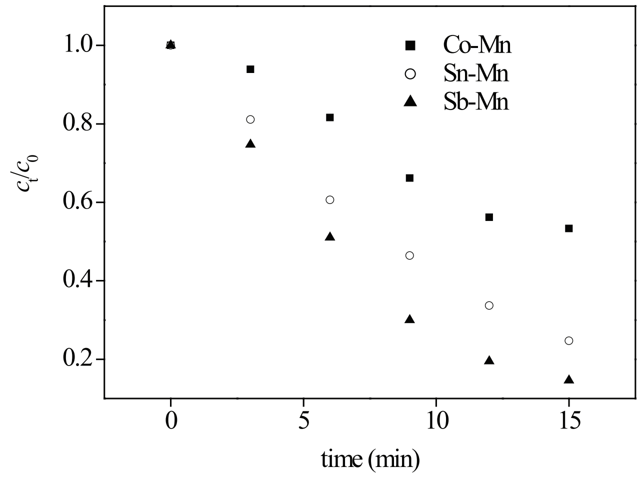

Fig. 7. Variation of normalized methyl orange concentration as a function of degradation time with different double-component catalysts. Experimental condition: 10.00 g particle electrode dose, 200 mL of solution, c_0 10.0 mg/L methyl orange, 12 g/L Na_2SO_4, and 9 V cell voltage.

3.6 min longer than that with the Mn single-component catalyst. The combination of Co and Mn components did not result in enhanced electrocatalytic performance; on the contrary, it weakened the electrocatalytic effect of the Mn catalyst which exhibited good catalytic activity. Therefore, the combination of any two components did not improve the electrocatalytic performance of the resulting double-component catalysts. The electrocatalytic performance of double-component catalysts could be effectively improved when synergetic effects were produced in the process of combining two catalytic components, which mainly depended on good electrocatalytic properties of each component.

3.3. Electrocatalytic performance of triple-component catalysts

We used 0.8 mol/L Sn, 0.1 mol/L Sb, and 0.4 mol/L Mn to investigate whether the electrocatalytic performance of the catalysts could be further improved through the combination of these three components. In addition, the effect of the loading order of the three catalytic components on the electrocatalytic performance of the resulting catalysts was also investigated.

Three different orders of the loading of Sn, Sb, and Mn components onto particle electrodes were investigated. In the first case, the Sb and Mn components were loaded onto particle electrodes first, followed by the loading of the Sn component; this catalyst was represented here as (Sb–Mn)–Sn. In the second case, the Sn and Mn components were loaded onto particle electrodes first, followed by the loading of the Sb component; this catalyst was represented as (Sn–Mn)–Sb. In the third case, the Sn, Sb, and Mn components were loaded onto particle electrodes simultaneously; this catalyst was represented as Sn–Sb–Mn. The triple-component catalysts supported on particle electrodes were used to degrade methyl orange, and the variations of normalized methyl orange concentration were presented in Fig. 8. Among the triple-component catalysts prepared in the above orders, the degradation rate of methyl orange with the Sn–Sb–Mn catalyst was slightly faster than that with the other two catalysts. We observed that, when the three components were loaded simultaneously, a large amount of gas was produced during the impregnation process and some black materials were produced inside and outside the container during the calcination process. However, these phenomena were not observed in the other two catalysts. These different reactions produced in the loading process with different orders might be responsible for the different electrocatalytic activities exhibited by the triple-component catalysts.

According to Table 1, the half-life with the Sn–Sb–Mn catalyst was 10.9 min, which was approximately 2.1 times greater than that with the Sb–Mn catalyst. The electrocatalytic performance of the triple-component catalyst was worse than that of corresponding double-component catalyst. More components of the catalyst might not yield better catalytic performance. Excessive catalytic components supported on particle electrodes weakened the electrocatalytic performance of the resulting catalysts and degraded their activity.

Fig. 9 shows the microscopic structure of particle electrodes with different catalysts. The Mn catalyst was loaded onto the surface of the particle electrodes in the form of granules, but failed to form fine and evenly dispersed particulates (Fig. 9(a)), whereas a good dispersion of the Sb catalyst could be observed in Fig. 9(b). These granules decreased the specific surface area of the electrode and were easily stripped from the electrode surface, which affected the catalytic stability of the Mn catalyst. When Sb component was added to the Mn catalyst, the surface of the resulting particle electrodes exhibited a homogeneous microstructure with fine particulates because of the interaction of the two components (Fig. 9(c)). The combination of Sb and Mn increased the number of pores on the electrode surface. Such porous structures play an important role when catalytic layers, which act as electron conduction paths from the catalyst to the solution bulk, are fabricated on electrode surfaces [39]. An increase in the number of pores is not only conducive to the mass-transfer diffusion of pollutants and powerful redox reagents during the electrolysis process but also increases the number of catalytically active sites. Therefore, the electrocatalytic performance of the Sb–Mn catalyst was superior to that of the corresponding single-component catalyst. However, when three components, that is, Sn, Sb, and Mn, were loaded onto particle electrodes simultaneously, the presence of excessive amounts of the catalyst components obviously changed the electrode surface structure, as shown in Fig. 9(d), where the microscopic structure of aggregates was evident. The agglomeration of the catalyst blocked the voids or pores in the electrode surface, which inhibited the transport of pollutants and products during the electrolysis process. Therefore, although the number of catalyst components was increased in the case of the Sn–Sb–Mn catalyst, its electrocatalytic performance was weakened. The half-life with the Sn–Sb–Mn catalyst was similar to that with the Mn single-component catalyst. The incorporation of an excessive amount of components did not further enhance the electrocatalytic performance of resulting catalyst; on the contrary, it increased the treatment cost and led to the waste of resources.

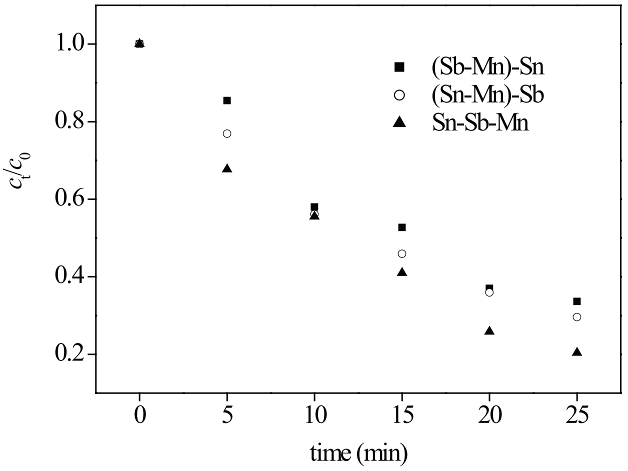

Fig. 8. Variation of normalized methyl orange concentration as a function of degradation time with different triple-component catalysts. Experimental condition: 10.00 g particle electrode dose, 200 mL of solution, c_0 10.0 mg/L methyl orange, 12 g/L Na_2SO_4, and 9 V cell voltage.

4. Conclusion

Transition metals and rare metals supported on particle electrodes served as catalysts in the electrolysis process.

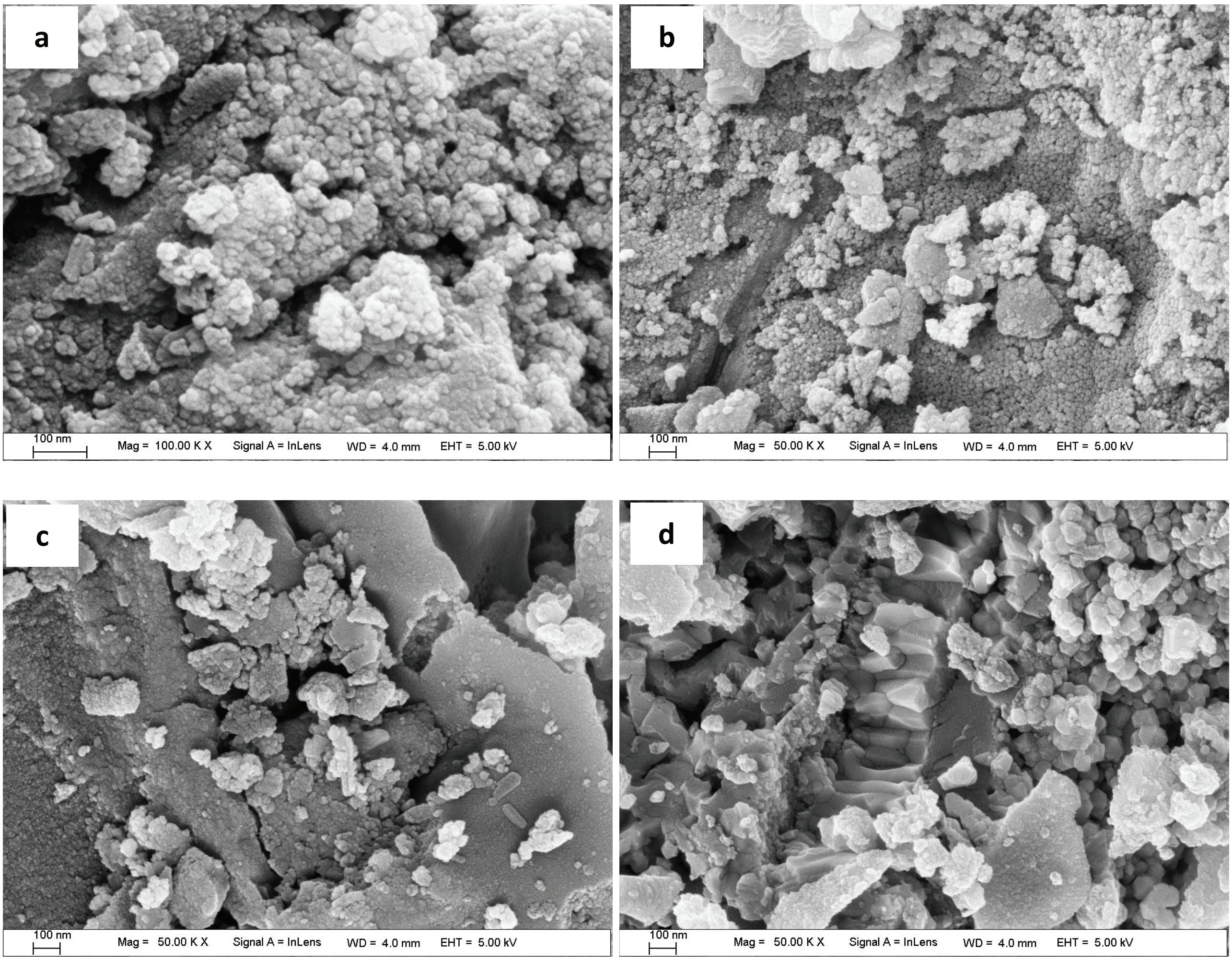

Fig. 9. SEM images of particle electrodes loaded with (a) Mn catalyst, (b) Sb catalyst, (c) Sb–Mn catalyst, and (d) Sn–Sb–Mn catalyst.

The electrocatalytic performance of single-component catalysts was closely related to their concentrations and the features of their electronic structures. Mn and Sb were observed to be excellent catalysts in this study. The combination of two catalytic components could enhance or counteract the electrocatalytic performance of the resulting double-component catalysts, depending on the electrocatalytic activity of each component. The double-component catalyst consisting of a combination of Sb and Mn exhibited improved electrocatalytic performance compared with that of Sb or Mn alone, whereas the combination of Co and Mn components weakened the electrocatalytic performance of the Mn catalyst. The combination of three catalytic components was not conducive for improving the electrocatalytic performance of catalysts because of agglomeration that occurred at the electrode surface.

Acknowledgments

This work was supported by Changzhou Science & Technology Program (CE20155054) and Jiangsu Province Key Laboratory of Environmental Engineering (KF2014010) for financial support.

References

[1] S.P. Balomenou, D. Tsiplakides, C.G. Vayenas, S. Poulston, V. Houel, P. Collier, A.G. Konstandopoulos, C. Agrafiotis, Electrochemical promotion in a monolith electrochemical plate reactor applied to simulated and real automotive pollution control, Top. Catal., 44 (2007) 481–486.

[2] R.M. Reis, J.A.F. Baio, F.L. Migliorini, R. da Silva Rocha, M.R. Baldan, N.G. Ferreira, M.R. de Vasconcelos Lanza, Degradation of dipyrone in an electrochemical flow-by reactor using anodes of boron-doped diamond (BDD) supported on titanium, J. Electroanal. Chem., 690 (2013) 89–95.

[3] R. Bhatnagar, H. Joshi, I.D. Mall, V.C. Srivastava, Electrochemical treatment of acrylic dye-bearing textile wastewater: optimization of operating parameters, Desal. Wat. Treat., 52 (2014) 111–122.

[4] E. Isarain-Chávez, C. Rosa, L.A. Godínez, E. Brillas, J.M. Peralta-Hernández, Comparative study of electrochemical water treatment processes for a tannery wastewater effluent, J. Electroanal. Chem., 713 (2014) 62–69.

[5] J. Jeong, J. Lee, Electrochemical oxidation in pigment wastewater treatment using a Ti/IrO$_2$ tube-type electrode, Desal. Wat. Treat., 4 (2009) 233–239.

[6] C. Carlesi, N.G. Ramírez, D. Carvajal, M.C. Hernández, D. Fino, Electrochemical treatment of bilge wastewater, Desal. Wat. Treat., 54 (2015) 1556–1562.

[7] A.K. Chopra, A.K. Sharma, Effect of electrochemical treatment on the COD removal from biologically treated municipal wastewater, Desal. Wat. Treat., 53 (2015) 41–47.

[8] Y. Xiong, C. He, T.C. An, X.H. Zhu, H.T. Karlsson, Removal of formic acid from wastewater using three-phase three-dimensional electrode reactor, Water Air Soil Pollut., 144 (2003) 67–79.

[9] N.N. Rao, M. Rohit, G. Nitin, P.N. Parameswaran, J.K. Astik, Kinetics of electrooxidation of landfill leachate in a three-dimensional carbon bed electrochemical reactor, Chemosphere, 76 (2009) 1206–1212.

[10] C.T. Wang, J.L. Hu, W.L. Chou, Y.M. Kuo, Removal of color from real dyeing wastewater by electro-Fenton technology using a three-dimensional graphite cathode, J. Hazard. Mater., 152 (2008) 601–606.

[11] L. Yan, H. Ma, B. Wang, Y. Wang, Y. Chen, Electrochemical treatment of petroleum refinery wastewater with three-dimensional multi-phase electrode, Desalination, 276 (2011) 397–402.

[12] C. Zhang, H. Lin, J. Chen, W. Zhang, Advanced treatment of biologically pretreated coking wastewater by a bipolar three-dimensional electrode reactor, Environ. Technol., 34 (2013) 2371–2376.

[13] B. Wang, W. Kong, H. Ma, Electrochemical treatment of paper mill wastewater using three-dimensional electrodes with Ti/Co/SnO_2-Sb_2O_5 anode, J. Hazard. Mater., 146 (2007) 295–301.

[14] M. Zhou, L. Lei, The role of activated carbon on the removal of p-nitrophenol in an integrated three-phase electrochemical reactor, Chemosphere, 65 (2006) 1197–1203.

[15] C.D. Vecitis, G. Gao, H. Liu, Electrochemical carbon nanotube filter for adsorption, desorption, and oxidation of aqueous dyes and anions, J. Phys. Chem. C, 115 (2011) 3621–3629.

[16] J. Yang, J. Wang, J.P. Jia, Improvement of electrochemical wastewater treatment through mass transfer in a seepage carbon nanotube electrode reactor, Environ. Sci. Technol., 43 (2009) 3796–3802.

[17] X. Wu, X. Yang, D. Wu, R.W. Fu, Feasibility study of using carbon aerogel as particle electrodes for decoloration of RBRX dye solution in a three-dimensional electrode reactor, Chem. Eng. J., 138 (2008) 47–54.

[18] D. Wu, R. Fu, M.S. Dresselhaus, G. Dresselhaus, Fabrication and nano-structure control of carbon aerogels via a microemulsion-templated sol-gel polymerization method, Carbon, 44 (2006) 675–681.

[19] L. Xu, H. Zhao, S. Shi, G. Zhang, J. Ni, Electrolytic treatment of C.I. acid orange 7 in aqueous solution using a three-dimensional electrode reactor, Dyes Pigm., 77 (2008) 158–164.

[20] M. Zhou, W. Fu, H. Gu, L. Lei, Nitrate removal from groundwater by a novel three-dimensional electrode biofilm reactor, Electrochim. Acta, 52 (2007) 6052–6059.

[21] Y. Xiong, C. He, H.T. Karlsson, X. Zhu, Performance of three-phase three-dimensional electrode reactor for the reduction of COD in simulated wastewater-containing phenol, Chemosphere, 50 (2003) 131–136.

[22] M.J. Lázaro, M.E. Gálvez, S. Artal, J.J. Palacios, R. Moliner, Preparation of steam-activated carbons as catalyst supports, J. Anal. Appl. Pyrolysis, 78 (2007) 301–315.

[23] C. Liu, Z. Shao, Z. Xiao, C. Liang, Hydrodeoxygenation of benzofuran over activated carbon supported Pt, Pd, and Pt–Pd catalysts, React. Kinet. Mech. Catal., 107 (2012) 393–404.

[24] C. Zhang, Y. Jiang, Y. Li, Z. Hu, L. Zhou, M. Zhou, Three-dimensional electrochemical process for wastewater treatment: a general review, Chem. Eng. J., 228 (2013) 455–467.

[25] S. Navalon, A. Dhakshinamoorthy, M. Alvaro, H. Garcia, Heterogeneous Fenton catalysts based on activated carbon and related materials, ChemSusChem, 4 (2011) 1712–1730.

[26] W. Kong, B. Wang, H. Ma, L. Gu, Electrochemical treatment of anionic surfactants in synthetic wastewater with three-dimensional electrodes, J. Hazard. Mater., 137 (2006) 1532–1537.

[27] G.P. Cao, F. Xu, S.A. Xia, Preparation of a composite particle electrode by electroless plating and its electrocatalytic performance in the decolorization of methyl orange dye solution, J. Braz. Chem. Soc., 24 (2013) 2050–2058.

[28] Y. Hardjono, H. Sun, H. Tian, C.E. Buckley, S. Wang, Synthesis of Co oxide doped carbon aerogel catalyst and catalytic performance in heterogeneous oxidation of phenol in water, Chem. Eng. J., 174 (2011) 376–382.

[29] G.P. Cao, J. Su, J.L. Lu, J.T. Zhang, Q.J. Liu, Preparation of Sb_2O_3-loaded activated carbon particle electrode and its electrocatalytic degradation of methyl orange in a three-dimensional electrode cell, J. Chin. Chem. Soc., 59 (2012) 583–588.

[30] M. Uğurlu, M.H. Karaoğlu, İ. Kula, Experimental investigation of chemical oxygen demand, lignin and phenol removal from paper mill effluents using three-phase three-dimensional electrode reactor, Pol. J. Environ. Stud., 15 (2006) 647–654.

[31] F. Duarte, V. Morais, F.J. Maldonado-Hódar, L.M. Madeira, Treatment of textile effluents by the heterogeneous Fenton process in a continuous packed-bed reactor using Fe/activated carbon as catalyst, Chem. Eng. J., 232 (2013) 34–41.

[32] E. Balanosky, J. Fernandez, J. Kiwi, A. Lopez, Degradation of membrane concentrates of the textile industry by Fenton like reactions in iron-free solutions at biocompatible pH values (pH ≈ 7–8), Water Sci. Technol., 40 (1999) 417–424.

[33] T.C. An, W.B. Zhang, G.Y. Li, J.M. Fu, G.Y. Sheng, Increase the degradation efficiency of organic pollutants with a radical scavenger (Cl^-) in a novel photoelectrocatalytic reactor, Chin. Chem. Lett., 15 (2004) 455–458.

[34] A. Isse, G. Berzi, L. Falciola, M. Rossi, P. Mussini, A. Gennaro, Electrocatalysis and electron transfer mechanisms in the reduction of organic halides at Ag, J. Appl. Electrochem., 39 (2009) 2217–2225.

[35] S.A. Mamuru, K.I. Ozoemena, T. Fukuda, N. Kobayashi, Iron(II) tetrakis(diaquaplatinum)-octacarboxyphthalocyanine supported on multi-walled carbon nanotube platform: an efficient functional material for enhancing electron transfer kinetics and electrocatalytic oxidation of formic acid, J. Mater. Chem., 20 (2010) 10705–10715.

[36] Y.Q. Cong, Z.C. Wu, Self-regeneration of activated carbon modified with palladium catalyst for electrochemical dechlorination, Chin. Chem. Lett., 18 (2007) 1013–1016.

[37] X.W. He, L.Y. Liu, J.W. Gong, J.B. Wang, Q. Qin, H. Wang, Electrochemical treatment of COD in biologically pretreated coking wastewater using Ti/RuO_2-IrO_2 electrodes combined with modified coke, J. Coal Sci. Eng., 17 (2011) 426–430.

[38] R.N. Singh, N.K. Singh, J.P. Singh, G. Balaji, N.S. Gajbhiye, Effect of partial substitution of Cr on electrocatalytic properties of $CoFe_2O_4$ towards O_2-evolution in alkaline medium, Int. J. Hydrogen Energy, 31 (2006) 701–707.

[39] F. Xie, H. Meng, P.K. Shen, Diffusion study in a novel three-dimensional electrode for direct methanol fuel cells, Electrochim. Acta, 53 (2008) 5039–5044.